

# Rain Streaks Removal in Images using Extended Generative Adversarial-based Deraining Framework

Subbarao Gogulamudi<sup>1\*</sup>

Research Scholar  
Department of Computer Science  
and Engineering  
Annamalai University, Annamalai  
Nagar, Chidambaram, Tamil Nadu  
608002-India

V. Mahalakshmi<sup>2</sup>

Assistant Professor  
Department of Computer Science  
and Engineering  
Annamalai University, Annamalai  
Nagar, Chidambaram, Tamil Nadu  
608002-India

Indraneel Sreeram<sup>3</sup>

Professor  
Department of Computer Science  
and Engineering  
St. Ann's College of Engineering and  
Technology, Chirala, Andhra  
Pradesh 523187-India

**Abstract**—The visual quality of photographs and videos can be negatively impacted by various weather conditions, such as snow, haze, or rain, affecting the quality of the images and videos. Such impacts may greatly affect outdoor vision systems that rely on image/video data. It has recently drawn a lot of interest to remove rain streaks from a single image. Several deep learning-based methods have been introduced to address the issue of removing rain streaks from a single image. Still, the efficiency of rain streak removal with enhanced quality is challenging. Hence, a novel deep-learning method is introduced for rain streak removal. The proposed Extended Generative Adversarial based De-raining (Ex\_GADerain) is the enhanced version of a traditional Generative adversarial network (GAN). The proposed Ex\_GADerain introduced a Self-Attention based Convolutional Capsule Bidirectional Network (SA-CCapBiNet) based generator for enhancing the rain streaks removal process. Also, the loss function estimation using the adversarial loss and the mean absolute error loss minimizes the information loss during training. The minimal information loss enhances the generalization capability of Ex\_GADerain, and hence the enhanced performance is acquired. The quality assessment of a derained image based on various assessment measures like SSIM, PSNR, RMSE, and DSSIM improved performance compared to the conventional rain streak removal methods. The maximal SSIM and PSNR acquired by the Ex\_GADerain are 0.9923 and 26.7052, respectively. The minimal RMSE and DSSIM acquired by the Ex\_GADerain are 0.9367 and 0.0051, respectively.

**Keywords**—Deep learning; rain streaks removal; image generation; quality measure; capsule network; adversarial learning

## I. INTRODUCTION

In recent scenarios, outdoor vision systems are mainly impacted by awful weather conditions, including rain [1]. Due to the large light scattering and motion velocities, the raindrops generally produce bright streaks in the captured images or videos through cameras [2]. Such conditions can highly influence the image's visual quality and also degrades outdoor vision systems' efficiency [3]. Also, it affects the efficacy of several computational vision mechanisms like event detection, scene analysis, and object detection and action recognition. Thus, such effects due to rain can be resolved by performing an automated rain streak removal process [4]. During rainy conditions, the streaks of rain generate haziness and blurring impact in images because of

light scattering [5]. Thus, effective approaches are highly needed for many practical applications to remove rain streaks from the captured images or videos [6].

The primary goal of raindrop removal is to reduce the rain effects, which has been analyzed extensively [7]. Computer vision techniques mainly consider a pure image as input for understanding a scene. However, the available rain streaks can blur the scene and degrade the performance of such techniques [8]. The major problem in deraining approaches is exploiting the necessary attributes of rain streaks and the pure image [9-12]. The model-based methods define the removal of rain streaks as an optimization issue [13]. It contains hand-crafted regularizers that mention the preceding knowledge of a solution, like repeatability, high-frequency probability of the rain streaks and the image's piecewise smoothness [14]. Nevertheless, such model-based mechanisms are unsuitable for rainy conditions since the degradation process can become more complicated [15]. To solve this issue, learning-based schemes are utilized to learn the essential attributes from the data like convolutional filters, stochastic distributions and Gaussian mixture models (GMMs) [16-18]. In recent years, deep learning techniques are becoming more popular for detection analysis. Such techniques can acquire the data characteristics by a trained deep neural network and with an effective representation capability, attaining appropriate outcomes and promoting the data to a large extent.

The conventional deep learning techniques face two difficulties while removing rain streaks. At first, the trained network's efficiency is mainly based on the training data. For instance, the deep detail network (DDN) is mainly focused on understanding the nonlinear mapping in detail layer to the rain streaks with straightforward network structures. Secondly, because of the complicated network design, several deep learning techniques can suffer [19]. The rain streaks removal methods are generally categorized based on the input type. Single-image methods are employed when the input is in image form. On the other hand, the single image techniques demand the need of image priors to regain the fundamental background scene, such as nonlocal self-similarity prior, dictionary-based sparse prior, GMM-based layer prior and low rank prior [20]. However, the existing methods face several challenges while eliminating rain streaks in the images.

### A. Research Questions

Some of the research questions concerning the proposed rain streak removal process are:

- 1) What is the need for including the noise removal technique through the filtering process?
- 2) How the efficient of the de-raining process enhanced with minimal computational complexity?
- 3) How the hybrid deep learning process generates the de-rained image by the generator module of the framework?
- 4) How the proposed method solves the problems faced by the existing methods?

The proposed study attempted to design a deep-learning model for removing rain streaks from input images. The major contributions of the research are:

- To develop a novel Extended Generative Adversarial based Deraining framework for eliminating awful rain streaks in input images.
- To attain needed information about rain streaks, a detailed layer is extracted in the proposed work with a hybrid filtering method.
- To obtain a de-rained image, a Self-Attention-based Convolutional Capsule Bidirectional Network is introduced in the generator block of the proposed framework.
- To evaluate different performance matrices for analyzing the efficacy of proposed framework with other existing methods.

## II. RELATED WORKS

Some recent studies on rain streaks removal through different techniques are described as follows: Wang et al. [21] developed a kernel-guided convolutional neural network (KGCNN) for eliminating rain streaks from a single image. This existing study involved three important steps for performing rain streak removal. The motion blur kernel was initially learned through a plain neural network named parameter network from the raining patch's detail layer. Next, the learned motion blur kernel was stretched into a degradation map with a similar spatial size as the rainy patch. Finally, the developed deraining network, along with the ResNet design, was trained with the help of stretched degradation map with the detail patches. The simulation analysis shows that the developed model obtained optimal performance; however, the overall processing time is enhanced.

Lin et al. [22] introduced a sequential dual attention network for removing rain streaks in a single image. For this purpose, the proposed study designed a framework named Sequential dual attention based Single image DeRaining deep Network (SSDRNet) model. An inherent correlation between rain streaks in a given input image should be more powerful than that among the rain streaks and background of an image. Thus, a two-stage learning mechanism was applied to acquire the spread of rain streaks in an image effectively. The developed two-stage deep neural network contains three

varied blocks such as multi-scale feature aggregation modules (MAMs), sequential dual attention blocks (SDABs) and residual dense blocks (RDBs). The details about rain streaks of the given image were learned through the developed two-stage mechanism and perfectly eliminates the noise. The simulation results show that the developed model achieved more appropriate SSIM and PSNR values than other methods.

Hettiarachchi et al. [23] introduced conditional generative adversarial networks (CGANet) to ignore rain streaks in the provided single images. This existing work utilized the adversarial loss in generative adversarial networks (GANs), which affords a new component to the loss function. It helps to maintain the outcome and assists in obtaining higher performance. Here, a generator network was employed to map the rainy images to de-rained images and a discriminator network was utilized to categorize actual and created de-rained images. Varied performance measures were employed to compute the efficacy of a developed model through synthesized and realistic images. The result analysis shows that the developed CGANet model has more potential than other competing methods.

Darney et al. [24] presented the rain streak removal process through a dictionary-based sparsity process with MCA estimation. This existing study introduced a sparse coding process to eliminate rain streaks by applying morphological component analysis (MCA). Using MCA, estimation, of course, becomes effortless to manage the rainy streaks in the provided images. Through sparse decomposition, removing and estimating each sample redundancy is highly feasible. To obtain optimal MSE and PSNR outcomes from the recovered images, the developed MCA scheme is integrated with the process of sparsity coding. Furthermore, the developed model attained reduced MSE value; however, the computational complexity is enhanced.

Chang et al. [25] presented the curriculum learning model for eliminating the rain streaks from input images. This study uses a direction and residual awareness network to ignore unwanted rain streaks to obtain a clear image. To prove the efficacy of a developed model, a statistical analysis was performed on the extended-scale actual rainy images and plotted that rain streaks in normal patches exhibit principal directionality. By applying a direction-aware network, the directionality property was endowed and helps to differentiate rain streaks from an image edge. Finally, residual aware block (RAB) was introduced to analyze the relationship between the image and residual. This model assisted in learning the balance parameters to emphasize the necessary image features and provided positive outcomes.

Yang et al. [26] devised a rain streak removal process using the fractal band learning based strategy based on self-supervised approach. Here, the discriminative features were extracted from the input rained image using the fractal band learning strategy. Besides, the regularization of the network was devised for enhancing the generalization capability of the network through the cross scale learning approach. The robustness of the model was depicted through the quantitative analysis. Still, the failure in considering the texture features degrades the performance of the model.

Wang et al. [27] designed a deep learning based image de-raining model, wherein the shared source residual module was incorporated in the conventional deep convolutional neural network for making the skip connection to solve the vanishing gradient issues. The computational overhead evaluated by the designed model was minimal with enhanced outcome. Still, the method degrades its performance compared to state of art methods due to the negative perception.

Ran et al. [28] introduced an image de-raining through the patch analysis. In this, patch analysis was devised based on the task driven strategy, wherein K-shot learning was utilized for removing the rain streaks from the image. Besides, the computational overhead of the designed model was minimized through the skip connections and accomplished superior outcome in removing the rain streaks. Still, the computational complexity of the model was higher.

Wang et al. [29] suggested a rain streak removal method using the joint depth estimation approach. Here, the dilated residual network was incorporated in the generator module of the conventional GAN network for generating the depth map to remove the rain streaks. The robustness of the model was proved based on both the quantitative and qualitative analysis. Still, the processing time of the model was higher.

### B. Problem Statement

The rainy weather environment highly influences the visibility of scene objects in acquired real-time images. Similarly, the visualization of a high-definition image captured by cameras degrades mainly under outdoor weather scenarios, including fog, snow and rain. These worst visual quality of real-time images can impact the nature of image surveillance, computer vision and multimedia applications. Hence, eliminating the rain streaks from the captured images is an essential demand in real-time multimedia applications. The rainy image generally defines the linear sum of the rain layer and a background image. In this case, restoring a blurred image due to rainy streaks is challenging because of several interconnection feasibilities among a specific image's rainy and background layers. Different techniques were developed to separate rainy streaks and clear images effectively. However, they failed to afford an appropriate performance because varied orientations and shapes of rain streaks degraded the images. Thus, to overcome limitations observed in previous studies, the proposed study introduced an effective rain streak removal mechanism by inspiring the higher efficiency of deep learning techniques. The proposed Ex\_GADerain approach removes the rain streaks from the image more efficiently by incorporating the novel SA-CCapBiNet in the generator module of the conventional GAN technique. Besides, the computation overhead is reduced through the detail layer extraction through the CGBiF.

## III. PROPOSED EX\_GADERAIN-BASED RAIN STREAKS REMOVAL

Varying weather conditions like rain, snow, fog, and haze influence the visual quality of outdoor captured images. Rain patterns generate more effects on the image's visual quality than others. In addition, the rain patterns also degrade the forward and background information of an image. Thus,

removing rain streaks from the captured images improves the necessity. Most recently, deep learning models have gained more attention for removing rain streaks in images. Therefore, the proposed study planned to design a deep learning mechanism called Extended Generative Adversarial based De-raining (Ex\_GADerain) framework to eliminate the rain streaks from the provided input images.

The proposed framework involves four stages: image acquisition, detail layer extraction, de-raining operation and classification. Initially, the input images are acquired from the publicly available dataset. The detail layer is extracted through Cross Guided Bilateral Filtering (CGBiF) method to attain essential information about rain streaks, removing unwanted noises. Then, the detail layer is provided as an input of the proposed Ex\_GADerain framework. This framework contains two important blocks: generator and discriminator. The generator block produces the de-rained image through a new Self-Attention based Convolutional Capsule Bidirectional Network (SA-CCapBiNet) model. The discriminator block of the GAN model classifies whether the generated de-rained image is real or fake. Thus, the proposed deep learning framework effectively removes the rain streaks from the input dataset images. The block diagram for Ex\_GADerain-based Rain Streaks Removal is depicted in Fig. 1.

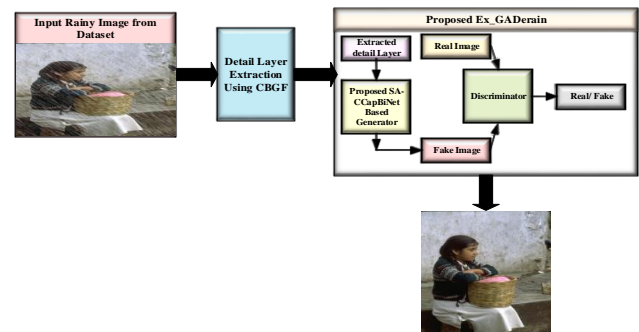


Fig. 1. Block diagram for Ex\_GADerain-based rain streaks removal.

### C. Image Acquisition

The rain streaks removal from the rained image using the proposed Ex\_GADerain acquires the input rain-streaked image from the rainy image dataset [26]. Let  $A$  be the dataset with a total of  $t$  images, from which  $f^{th}$  image is taken for processing the proposed Ex\_GADerain. It is expressed as,

$$A = \{A_1, A_2, \dots, A_f, \dots, A_t\} \quad (1)$$

Where, the  $f^{th}$  image in the dataset is indicated as  $A_f$ .

### D. Detail Layer Extraction

The detail layer extraction is devised using cross guided bilateral filter (CGBF). In this, a guided image with weight and robust properties is utilized along with the bilateral filter. The CGBF comprises two different filters for performing filtering and kernel identification. In the traditional cross-bilateral filter (CBF), nearby pixels' geometric closeness and gray-level similarities are considered in the image to perform the filtering operation. In contrast, the guided bilateral filter

(GBF) uses a guided image indication based on similar pixels in the neighbourhood concerning an image. The hybridization of characteristic behaviour of both the GBF and CBF constitutes the CGBF [31]. The CGBF-based detail layer extraction is depicted in Fig. 2.

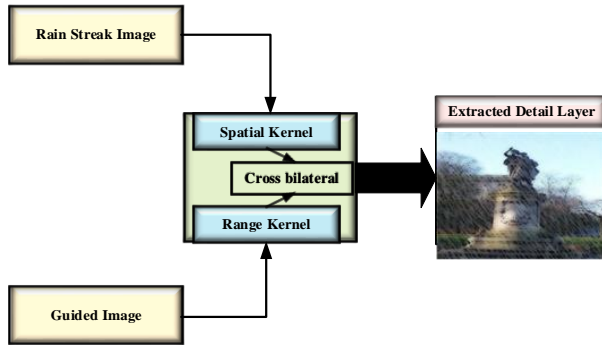


Fig. 2. CGBF-based detail layer extraction.

The outcome of a CGBF-based detail layer extraction is formulated as,

$$d_{DLE}(M,N) = P_{DLE} = \frac{1}{W_{M,N} \sum_{M,N \in W_{M,N}} S \cdot Y_{\sigma k}(|M-N|) Y_{\sigma g}(|P(M)-P(N)|) P(N)} I_{M,N} V_{M,N} + J_{M,N} \quad (2)$$

The outcome of a CGBF filtering is the detail layer extraction, which is represented as  $d_{DLE}(M,N)$ .  $M$  and  $N$  Refers to the adjacent pixels in the location  $P(M)$  and  $P(N)$ , and the guided image is indicated as  $S$ . The range and spatial kernel functions concerning the CGBF are formulated as:

$$Y_{\sigma k}(|M-N|) = e^{-\frac{|M-N|^2}{2\sigma k^2}} \quad (3)$$

$$Y_{\sigma g}(|P(M)-P(N)|) = e^{-\frac{|P(M)-P(N)|^2}{2\sigma g^2}} \quad (4)$$

Where, the spatial kernel function is notated as  $Y_{\sigma k}$ , and the range function is notated as  $Y_{\sigma g}$ . The constraints are notated as  $\sigma g$  and  $\sigma k$  respectively. The smoothing of an image is employed for the reduction of error based on coefficients of the guided filter  $I_{M,N}$  and  $J_{M,N}$  and is formulated as,

$$I_{M,N} = \frac{\sum_{i \in W_{M,N}} V^i U^i - V^{M,N} U^i}{\sigma_{M,N}^2 + \gamma} \quad (5)$$

$$J_{M,N} = U^i - I_{M,N} V^{M,N} \quad (6)$$

Where, guided and original image's mean indicated as  $V^i$  and  $U^i$  respectively. The window function is indicated as  $W$ , and the regularization constant is indicated as  $\gamma$ . The variance

is notated as  $\sigma_{M,N}^2$ . The extracted detail layer is fed into the Ex\_GADerain module for de-raining the image and classification.

### E. Ex\_GADerain-based Rain Streaks Removal

The rain streaks image filtered by the cross-guided bilateral filter is fed into the proposed Extended Generative Adversarial based Deraining (Ex\_GADerain) for obtaining the de-rained image. The proposed Ex\_GADerain is the improved version of traditional GAN. The GAN comprises networks, adversarial and generative components, each with specific functions.

a) *Networks*: The networks are utilized for training; hence, deep neural network (DNN) is utilized in GAN for learning.

b) *Adversarial*: The learning of a network is devised by the adversarial settings of a GAN.

c) *Generative*: The generation of data is performed by the generative model through the probabilistic approach.

GAN's work utilizes various network learning approaches termed discriminator and generator to make better decisions. Initially, GAN's generator produces a fake outcome based on the given input to confuse the discriminator. Hence, the role of a discriminator is to identify the original sample from the combined original and fake samples. Generating a fake outcome and identifying an original sample by the discriminator continues repetitively until optimal learning [32]. The proposed Ex\_GADerain is depicted in Fig. 3.

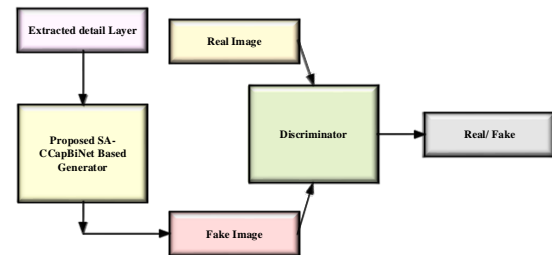


Fig. 3. Proposed Ex\_GADerain.

The reason behind the consideration of GAN for acquiring the de-rained image is its high-quality image outcome for performing the image processing tasks. Here, the generator is utilized for generating the de-rained image. Hence, the rain streaks removal process is further enhanced by incorporating Self-Attention based Capsule Bidirectional Network (SA-CCapBiNet) model on the generator side. The proposed SA-CCapBiNet is designed by hybridizing the Convolutional Capsule Network, Bidirectional Long Short Term Memory (BiLSTM), and the self-attention module. The illustration of a proposed SA-CCapBiNet for a generator is portrayed in Fig. 4.

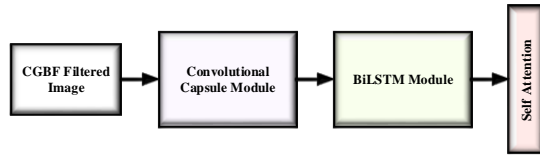


Fig. 4. Architecture of proposed SA-CCapBiNet for generator.

1) *Proposed SA-CCapBiNet-based generator module*: The traditional GAN utilizes DNN in the generator module to generate real and fake images. In the proposed Ex\_GADerain technique of de-raining the rained image, SA-CCapBiNet is utilized in the generator for generation images. The newly devised SA-CCapBiNet is the hybridized structure of Convolutional Capsule Network (CCap), Bidirectional Long short term memory (BiLSTM), and self-attention mechanism. A detailed description is given below.

2) *Convolutional capsule network (CCap)*: The convolutional neural network (CNN) is a deep learning architecture commonly utilized for image processing tasks due to its promising solution. The two unique features utilized by CNN have shared weights and local connections. In addition, the parameter reduction is employed by CNN through the replicated weighting criteria. The outcome of the CNN is expressed as,

$$y_q^h = a \left( \sum_{p=1}^{F_{map}} y_p^{h-1} * r_{pq}^h + e_q^h \right) \quad (7)$$

$$a(y) = \max(0, y) \quad (8)$$

Where, the outcome of a past iteration  $h-1$  concerning the  $p^{th}$  feature is indicated as  $y_p^{h-1}$ , the total features are notated as  $F_{map}$ , the  $q^{th}$  feature concerning the current iteration  $h$  is expressed as  $y_q^h$ , and the activation is notated as  $a(\cdot)$ . The convolution operation is indicated as  $*$ .

a) *Activation*: Rectified Linear Unit (ReLU) is utilized to transform the features nonlinearly to learn the complex features more accurately.

CNN's pooling operation is utilized for feature reduction, which causes information to be lost. Also, the CNN limits performance by changing scale, translational and rotational variance, but superior performance is acquired with the CapsuleNet. Thus, the combined Convolutional Capsule Network (CCap) is utilized in the proposed SA-CCapBiNet method.

b) *CapsuleNet*: The input to CapsuleNet is CNN's feature vector output. The CapsuleNet output is estimated using the Squashing function and is formulated as follows,

$$w_q = \frac{\|u_q\|^2}{\alpha + \|u_q\|^2} \frac{u_q}{\|u_q\|} \quad (9)$$

where,  $u_q$  refers to the input, the activation function is indicated as squashing function and is represented as  $w_q$ , in which the long vector is shrunken into the required length based on  $\alpha$  and the short vector is shrunken to the length zero. The CapsuleNet acquires the input as,

$$u_q = \sum_p s_{pq} Wei_{pq} v_p \quad (10)$$

Where, the weight factor is notated as  $Wei_{pq}$ , and the outcome of a capsule is indicated as  $v_p$ .

Then, an expression for the coupling coefficient  $s_{pq}$  is formulated as,

$$s_{pq} = \frac{\exp(x_{pq})}{\sum_n x_{pn}} \quad (11)$$

Where, the probabilities of two coupled capsules are notated as  $x_{pq}$  and  $x_{pn}$  respectively.

The coupling coefficient is updated iteratively based on dynamic routing. The outcome of a subsequent layer is shared with the parent layer for each capsule's output, which is called dynamic routing. Here, the weight updation based on dynamic routing considers the adjacent capsule for enhancing the similarity between two coefficients. Thus, the combined CCap network replaces the single neuron with the neuron vector to enhance rain streaks removal efficiency. The features mapped using the CCap are fed into the BiLSTM to generate fake images to confuse the discriminator. The architecture of a CCap Network is depicted in Fig. 5.

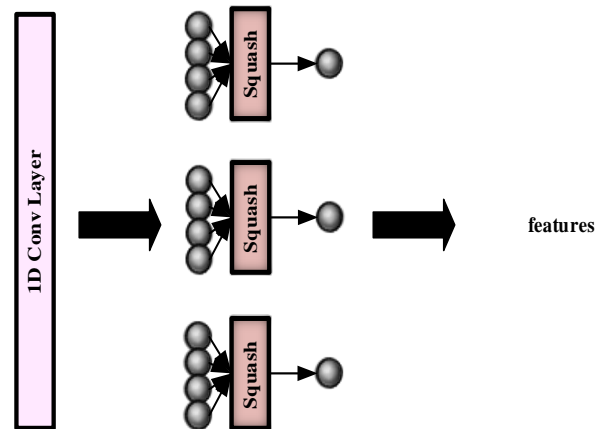


Fig. 5. Architecture of convolutional CapsuleNet (CCap).

3) *BiLSTM*: The outcome of CCap is taken as input to the BiLSTM module for capturing the long-term dependency information. The BiLSTM comprises several LSTM cells, wherein a gating mechanism is utilized to capture the essential

attribute mapping. The architecture of BiLSTM is depicted in Fig. 6(a), wherein the LSTM cell is portrayed in Fig. 6(b).

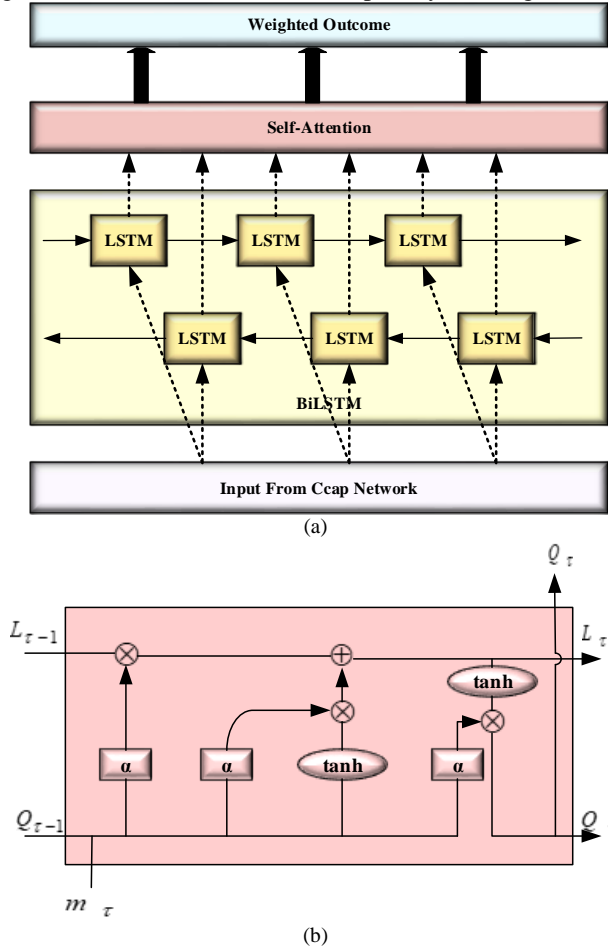


Fig. 6. Architecture of (a) BiLSTM and (b) LSTM cell.

a) *LSTM*: A recurrent neural network (RNN) with the memory unit constitutes the LSTM and is designed to overcome the issues concerning the vanishing gradient that limits the generalization capability. The gates and cell functioning are the major concept utilized in LSTM for making decisions. Cell state is utilized to maintain the information for further processing, which helps to minimize the vanishing gradient issue.

b) *Cell State*: The memory cell of LSTM constitutes the cell state, wherein the decision concerning the information removal or insertion is devised using the gating mechanism. The functioning is performed through sigmoid and point-wise multiplication for information maintenance. The cell state result is either '1' or '0', in which the information removal is devised for zero outcomes and the information maintenance is devised for the outcome '1'. Here,  $\tilde{L}_\tau$  refers to the cell state and its new state is notated as  $L_\tau$ . The formulation for the cell state based on the hidden state and input is expressed as,

$$\tilde{L}_\tau = \tanh(Z_L[Q_{\tau-1}, m_\tau] + X_L) \quad (12)$$

$$L_\tau = G_\tau * Q_{\tau-1} + R_\tau * \tilde{L}_\tau \quad (13)$$

Where,  $X_L$  refers to the bias and  $Z_L$  refers to the weight, hidden state is notated as  $Q_{\tau-1}$ , the input message is indicated as  $m_\tau$ , forget gate's outcome is indicated as  $G_\tau$ , and the outcome of the input gate is indicated as  $R_\tau$ .

c) *Forget Gate*: The less informative features are removed by the forget gate, which is evaluated as,

$$G_\tau = \alpha(Z_G[Q_{\tau-1}, m_\tau] + X_G) \quad (14)$$

Where, the sigmoid activation is indicated as  $\alpha$  the bias and weight concerning the forget gate are notated as  $X_G$  and  $Z_G$  respectively. Here, the outcome of a sigmoid function decides whether the information is remembered or forgotten.

d) *Input Gate*: The role of an input gate is to regulate the information that needs to be included in the cell state by using the sigmoid function. Feature filtering is employed for information maintenance by considering the input and hidden state. The sigmoid gate devises the filtering of information, and the expression for the input gate outcome is,

$$R_\tau = \alpha(Z_R[m_\tau, Q_{\tau-1}] + X_R) \quad (15)$$

Where, the outcome of an input gate is indicated as, and the bias and weight concerning the input gate are notated as  $X_R$  and  $Z_R$ , respectively.

e) *Output Gate*: The feature vector generation using the tanh function and filtering using the sigmoid function are devised in the output gate for better decision-making. The outcome of an output gate is,

$$G_\tau = \alpha(Z_G[Q_{\tau-1}, m_\tau] + X_G) \quad (16)$$

$$Q_\tau = D_\tau * \tanh(L_\tau) \quad (17)$$

Where, the outcome of a gate is indicated as  $G_\tau$ , and the bias and weight concerning the input gate are notated as  $X_G$  and  $Z_G$  respectively.

f) *BiLSTM*: The information processing is devised in only one direction by the existing LSTM; hence, considering the past information is impossible. Thus, considering previous information, backward processing is essential, accomplished through backward information processing. Let  $\vec{P}_\tau$  be the

forward direction-based processing and  $\overleftarrow{P}_\tau$  be the backward direction processing of the BiLSTM. The architecture with both directional behaviours is depicted in Fig. 5. The outcome of BiLSTM is formulated as,

$$P_\tau = \vec{P}_\tau \oplus \overleftarrow{P}_\tau \quad (18)$$

Where, the outcome of BiLSTM is notated as  $P_\tau$ , and the summation operation is notated as  $\oplus$ . The outcome of BiLSTM is more efficient due to considering both the subsequent and preceding information.

g) *Self-attention*: The assignment of weights among the extracted features is devised in the self-attention module. Here, the weights are employed for the features extracted by the BiLSTM, wherein the highest weight is assigned for the most significant attributes. The correlation between the currently hidden and high-dimensional vectors is utilized for weighting the attributes. The hidden vector formulation is expressed as,

$$\mu_{\tau} = \tanh(Z_z * Q_{\tau} + X_z) \quad (19)$$

Where, the hidden vector is notated as  $\mu_{\tau}$ , the hidden state is indicated as  $Q_{\tau}$ , the bias is indicated as  $X_z$  and the weight is notated as  $Z_z$ . Then, the outcome of an attention module is expressed as,

$$Attn = \sum_{\tau} \eta_{\tau} * Q_{\tau} \quad (20)$$

Where, the variable  $\eta_{\tau}$  is calculated as,

$$\eta_{\tau} = \frac{\exp(\mu_{\tau} * \mu_z)}{\sum_{\tau} \exp(\mu_{\tau} * \mu_z)} \quad (21)$$

Here, the high dimensional feature is indicated as  $\mu_z$ . An outcome of the self-attention module is the de-rained image.

4) *Generator-discriminator operation*: Here, the proposed SA-CCapBiNet generator acquires the input data  $p(m)$  and the noisy variable  $p(c)$ , in which the input is the rain streaks image. While performing the rain streaks removal process, the attributes like texture information and higher order colour are maintained during the image translation.

a) *Loss Function*: The loss of a proposed Ex\_GADerain is minimized through the min-max optimization issue and is expressed as,

$$MIN^G MAX^D = K_{m \sim p(m)} |\log D(m)| + K_{c \sim p(c)} |\log(1 - G(c))| \quad (22)$$

Where, the discriminator is indicated as  $D$ , the generator is indicated as  $G$ , the expectation operator is indicated as  $K$ , the input rain streak image is indicated as  $p(m)$  and the noisy image is indicated as  $p(c)$ . The role of a discriminator is to correctly identify the fake image generated by the generator and try to maximize  $\log D(m)$ . In contrast to the generator, SA-CCapBiNet tries to minimize the  $\log(1 - G(c))$ . Thus, the min-max optimization is devised in GAN for enhancing the image de-raining process.

In addition to the adversarial loss function, the mean absolute error is included for generating the blurred image. Thus, the loss function of the proposed Ex\_GADerain is expressed as,

$$L_{MAE} = K_{m,b,c} \left[ \|m - G(c,b)\| \right] \quad (23)$$

Where, the mean absolute error is notated as  $L_{MAE}$ , the generated image is indicated as  $G(c,b)$  in the region  $(m,b,c)$ . Then, the total loss of a proposed Ex\_GADerain is formulated as,

$$L_{Total} = L_{Ex\_GADerain}(G.D) + \beta L_{MAE}(G) \quad (24)$$

Where, the parameter utilized for controlling the weights is indicated as  $\beta$ .

Thus, learning based on the loss function enhances the accuracy of a de-raining process and provides an efficient outcome.

#### F. Classification of Input Image

The outcome of the self-attention module is utilized for decision-making regarding whether the concerning input image is rained image or not. For this, this softmax activation is utilized and is formulated as,

$$C = \text{soft max}(Z_c s + X_c) \quad (25)$$

Where, the classification outcome is indicated as  $C$ , the input vector is indicated as  $s$ , the bias is indicated as  $X_c$  and the weight is notated as  $Z_c$ .

Hence, the outcome of a proposed Ex\_GADerain is the classification of an input image as rained or not.

## IV. RESULTS AND DISCUSSION

The proposed Ex\_GADerain technique is analyzed by implementing the proposed methodology in PYTHON programming language using an 8GB RAM PC with Windows 10OS. The experimental outcome and various assessments are devised to portray the excellence of the Ex\_GADerain method.

a) *Dataset Used*: The rainy image dataset [30] analyses the proposed method's performance. The dataset has 1000 normal images with 14 rainy images with different magnitudes and orientations of rain streaks. The rainy image was generated using photoshop.

#### A. Experimental Outcome

The experimental outcome of a proposed Ex\_GADerain is illustrated in Fig. 7, wherein the rain-streaked image is portrayed in Fig. 7(a), the detail layer extracted image is portrayed in Fig. 7(b) and the de-rained image is portrayed in Fig. 7(c).





Fig. 7. Experimental outcome of Ex\_GADerain: (a) Input rainy Image, (b) Detail layer extraction and (c) De-rained image

Fig. 7 shows that removing the rain streaks using the proposed Ex\_GADerain technique obtained a visually better outcome. Still, the quality of a de-rained image is analyzed through image quality assessment measures.

### B. Image Quality Assessment

The outcome of a proposed Ex\_GADerain-based de-rained image is assessed based on various image quality assessment measures like structural similarity index measure (SSIM), Dissimilarity index measure (DSSIM), peak signal to noise ratio (PSNR), and root mean square error (RMSE).

1) *Structural similarity*: The similarity between the de-rained images acquired by the proposed Ex\_GADerain and the original image is measured through the SSIM measure. By setting various windows, the quality of an image is measured. Let's consider a window size  $B \times B$  for both the de-rained and original images. Then, the expression for the SSIM is formulated as,

$$SSIM_{t,o} = \frac{(2M_t M_o + s_1)(2\sigma_{to} + s_2)}{(M_t^2 + M_o^2 + s_1)(\sigma_t^2 + \sigma_o^2 + s_2)} \quad (26)$$

Where, the mean concerning the de-rained image is indicated as  $M_t$ , the mean concerning the original image is indicated as  $M_o$ , and the covariance is notated as  $\sigma_{to}$ . The variance for the de-rained and original image is notated as  $\sigma_t$  and  $\sigma_o$  respectively. The stabilization factors are notated as  $s_1$  and  $s_2$ , respectively. The analysis based on the similarity index of a proposed Ex\_GADerain method is depicted in Fig. 8. The similarity between the derained outcomes of the proposed Ex\_GADerain with an original image with 50% learning and 40 epoch is 0.7015, which is 0.9697 with 90% of learning data. The similarity value with 90% learning data is

closer to the maximal value 1, which depicts the excellence of a proposed method in removing the rain streaks in a rainy image. The detailed analysis of Ex\_GADerain based on SSIM is depicted in Table I.

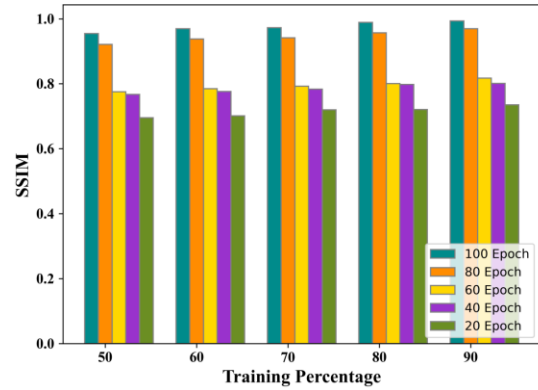


Fig. 8. Analysis of Ex\_GADerain based on SSIM.

TABLE I. ANALYSIS OF EX\_GADERAIN BASED ON SSIM

Epoch	Training Data				
	50	60	70	80	90
20	0.6955	0.7673	0.7756	0.9212	0.9545
40	0.7015	0.7765	0.7849	0.9378	0.9697
60	0.7197	0.7837	0.7926	0.9415	0.9726
80	0.7209	0.798	0.8005	0.9569	0.9888
100	0.7353	0.8009	0.8175	0.9695	0.9935

2) *Dissimilarity measure*: The dissimilarity between the de-rained image and an original image is measured through DSSIM. The formulation for finding the DSSIM is expressed as,

$$DSSIM_{t,o} = \frac{1 - SSIM_{t,o}}{2} \quad (27)$$

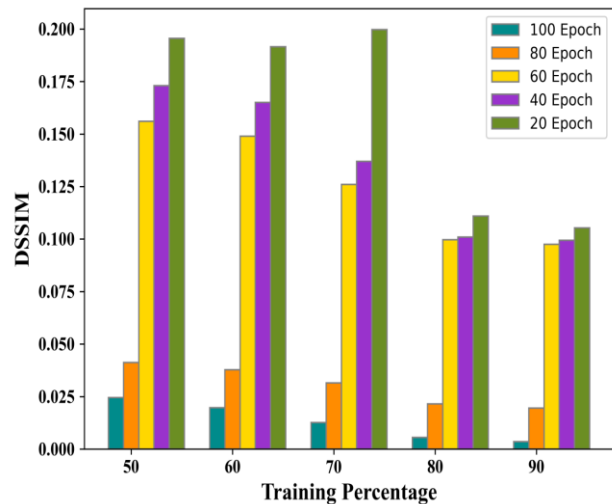


Fig. 9. Analysis of Ex\_GADerain based on DSSIM.

TABLE II. ANALYSIS OF EX\_GADERAIN BASED ON DSSIM

Epoch	Training Data				
	50	60	70	80	90
20	0.1955	0.173	0.156	0.0412	0.0245
40	0.1915	0.165	0.149	0.0378	0.0197
60	0.1997	0.137	0.126	0.0315	0.0126
80	0.1109	0.1009	0.0997	0.055	0.0215
100	0.1053	0.0994	0.0975	0.0195	0.0035

Where, the dissimilarity is notated as  $DSSIM_{t,o}$ . The analysis of Ex\_GADerain based on DSSIM is portrayed in Fig. 9. With 60% of data learning and 20 epochs, the DSSIM evaluated by the Ex\_GADerain is 0.173, which is 0.0994 for 100 epochs with the same training data. Thus, the epoch value enhancement improves the de-raining process by reducing the dissimilarity between the images. Likewise, for 70% of learning data and 80 epochs evaluated, the DSSIM of 0.0997 is 0.0215 with 90% of learning data. Thus, the increased amount of learning data minimizes the image's dissimilarity, indicating the more accurate removal of rain streaks. Thus, the minimal value of dissimilarity is acquired with higher learning data and epoch values. Also, the minimal DSSIM between the de-rained and original image depicts the better outcome of the proposed Ex\_GADerain method. The detailed analysis of Ex\_GADerain based on DSSIM is portrayed in Table II.

3) *Peak signal-to-noise ratio*: The reconstructed image quality from the rainy image based on the noise level is measured through the PSNR. The ratio between the original image and the noise evaluated based on the error defines the PSNR. Here, the error measure of the de-rained image is evaluated through the mean square error (MSE). Then, the formulation of PSNR is expressed as,

$$PSNR = 10 \log_{10} \frac{Value_{peak}}{MSE} \quad (28)$$

Where, the peak value of a de-rained image is notated as  $Value_{peak}$ . The MSE is formulated as,

$$MSE = \frac{\sum_{R,C} (I_t(R,C) - I_o(R,C))}{R * C} \quad (29)$$

Where, the number of rows is indicated as  $R$ , the number of columns is indicated as  $C$ , and the intensity of an original and derained image is notated as  $I_o(R,C)$  and  $I_t(R,C)$ , respectively. The analysis based on PSNR is depicted in Fig. 10. The maximal PSNR acquired by the Ex\_GADerain is 26.4052 with epoch 80 and 80% of learning data, which is 26.5457 with 90% of learning data with epoch 80. Here, the PSNR value also elevates with the epoch and learning data percentage enhancement. The larger value of PSNR measured in decibels depicts a better outcome, and the detailed analysis is portrayed in Table III.

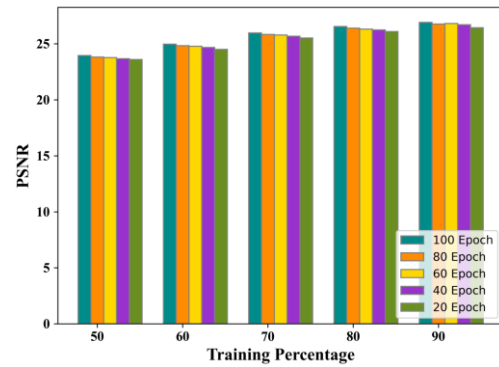


Fig. 10. Analysis of Ex\_GADerain based on PSNR.

TABLE III. ANALYSIS OF EX\_GADERAIN BASED ON PSNR

Epoch	Training Data				
	50	60	70	80	90
20	23.5955	23.6673	23.7756	23.8212	23.9545
40	24.5015	24.6765	24.7849	24.8378	24.9697
60	25.5197	25.6837	25.7926	25.8415	25.9726
80	26.0962	26.2372	26.3155	26.4052	26.5457
100	26.4353	26.7009	26.8175	26.7695	26.9135

4) *Root mean square error*: RMSE is an error measure that evaluates the error in the de-rained outcome based on the MSE. The formulation for the RMSE is defined as,

$$RMSE = \sqrt{MSE} \quad (30)$$

The analysis based on RMSE is depicted in Fig. 11. The RMSE evaluated by the Ex\_GADerain method is 2.3955 with 20 epochs and 50% learning data, 2.1573 with learning data of 60%, 1.7312 with learning data of 80%, and 0.9445 with learning data of 90%. The analysis shows that the error gets minimized with more information learning. The higher amount of data the classifier learns enhances the generalization capability and minimizes the error in removing the rain streaks. The difference between the original and derained image based on the error magnitude accomplished minimal error that indicates the enhanced quality of the rain streaks removal process. The detailed analysis is depicted in Table IV.

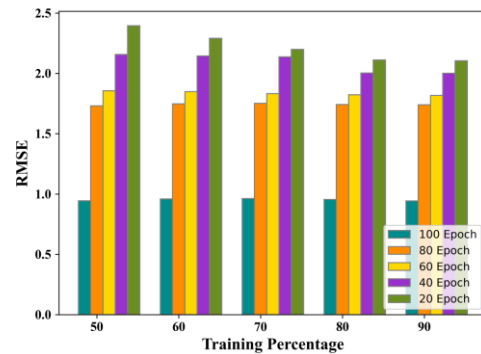


Fig. 11. Analysis of Ex\_GADerain based on RMSE.

TABLE IV. ANALYSIS OF EX\_GADERAIN BASED ON RMSE

Epoch	Training Data				
	50	60	70	80	90
20	2.3955	2.1573	1.856	1.7312	0.9445
40	2.2915	2.145	1.849	1.7478	0.9597
60	2.1997	2.137	1.8326	1.7515	0.9626
80	2.1109	2.0031	1.8223	1.7421	0.9545
100	2.1053	2.0009	1.8175	1.7395	0.9435

C. Comparative Analysis

The existing image de-raining techniques like CGAN [21], KGCNN [22] and SSDRNet [23] are compared with the proposed Ex\_GADerain method to depict the performance enhancement. Fig. 12 depicts the comparative analysis. The SSIM estimated by the Ex\_GADerain method is 0.9562 with 60% of data learning, which is higher than the conventional methods. Conventional KGCNN acquired the SSIM of 0.9336, CGAN of 0.7796 and SSDRNet of 0.7736, respectively. The dissimilarity measures of the EX\_GADerain method is 0.0126 with 70% of training data; the traditional methods like KGCNN, CGAN, and SSDRNet accomplished the higher DSSIM value of 0.0315, 0.126, and 0.147, respectively. The error estimation based on RMSE estimated by the Ex\_GADerain method is 0.9545 with 80% of training data, which is minimal compared to the traditional methods like KGCNN, CGAN and SSDRNet that acquired the RMSE value of 1.7421, 1.8223, and 2.0031 respectively. The maximal PSNR acquired by the Ex\_GADerain method is 25.8552, with 50% of data learning. The traditional KGCNN, CGAN and SSDRNet methods acquired the minimal PSNR of 25.6549, 24.2887, and 23.9778, respectively. Thus, the Ex\_GADerain method accomplished superior performance for all quality measures.

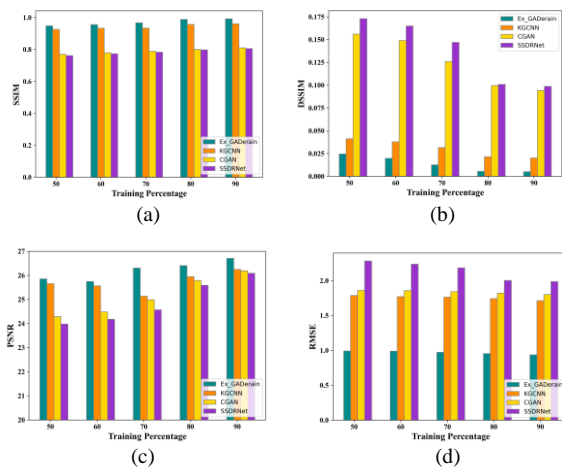


Fig. 12. Comparison in terms of (a) SSIM, (b) DSSIM, (c) PSNR and (d) RMSE.

D. Analysis based on the Classification

The detection of the rainy or non-rainy input image is devised by the proposed Ex\_GADerain technique prior to the rain streaks removal.

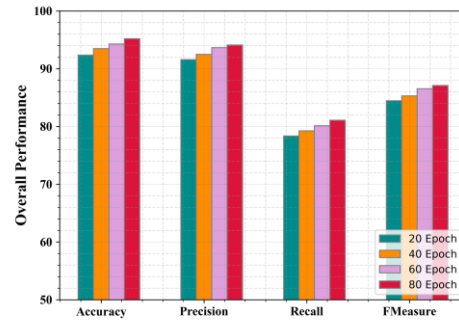


Fig. 13. Analysis based on the classification.

TABLE V. OVERALL PERFORMANCE ANALYSIS

Metrics/ Epoch	20	40	60	80
Accuracy	92.3576	93.479	94.286	95.1852
Recall	91.5763	92.482	93.655	94.1032
Precision	78.3517	79.252	80.127	81.0779
F-measure	84.4512	85.296	86.542	87.1063

The image detected as rainy is utilized for removing the rainy streaks to acquire the de-rained image. The outcome of the classification task based on the performance measures like accuracy, precision, recall and F-Measure is portrayed in Fig. 13. The outcome based on the classification task based on overall performance analyzed in Table V.

1) Accuracy and loss: The accuracy and loss analysis of a proposed Ex\_GADerain method based on the testing and training data by varying the epoch is depicted in Fig. 14. The accuracy of training is higher compared to the testing process. Likewise, the loss concerning the testing process is higher than the training process.

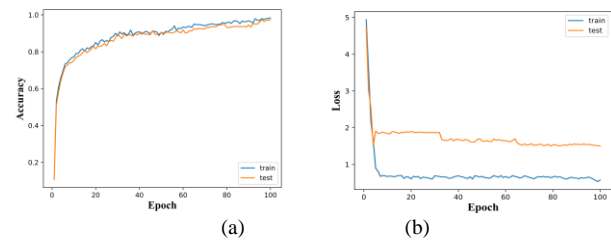


Fig. 14. Accuracy and loss analysis: (a) Accuracy and (b) Loss.

E. Complexity Analysis

The complexity analysis of a proposed Ex\_GADerain with the conventional methods is depicted in Fig. 15. While training the data, the time complexity of the Ex\_GADerain method is 65.34ms, which is 6.76%, 3.13%, and 1.21% improved performance compared to the traditional KGCNN, CGAN, and SSDRNet. Likewise, the time complexity of rain streaks removal methods while testing is 12.56ms, 13.91ms, 14.89ms, and 15.78ms for Ex\_GADerain, KGCNN, CGAN, and SSDRNet methods. Here, the proposed Ex\_GADerain acquired minimal time complexity compared to the traditional testing and training methods.

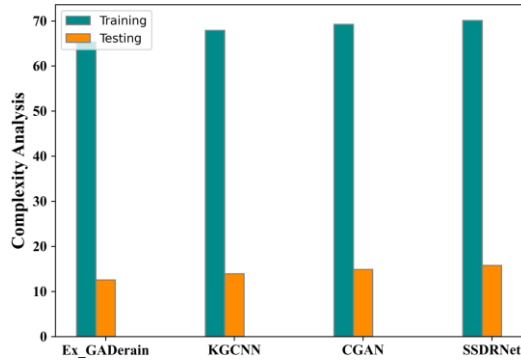


Fig. 15. Complexity analysis.

### F. Comparative Discussion

The best outcome of Ex\_GADerain based on various assessment measures along with the traditional KGCNN, CGAN and SSDRNet is depicted in Table VI. The maximal similarity of the de-rained image with the original image evaluated by the Ex\_GADerain is 0.9923, which is 3.13%, 18.35%, and 18.84% enhanced performance compared to conventional KGCNN, CGAN and SSDRNet methods. The maximal PSNR evaluated by the Ex\_GADerain is 26.752, 1.72%, 1.93%, and 2.31% enhanced performance compared to conventional KGCNN, CGAN and SSDRNet methods. The minimal RMSE acquired by Ex\_GADerain is 0.9367, which is 45.30%, 48.03%, and 52.87% enhanced performance compared to conventional KGCNN, CGAN and SSDRNet methods. The minimal DSSIM acquired by Ex\_GADerain is 0.0051, which is 74.63%, 94.59%, and 94.83% enhanced performance compared to conventional KGCNN, CGAN and SSDRNet methods. Here, Ex\_GADerain accomplished excellent performance compared to the conventional rain streaks removal methods.

TABLE VI. COMPARATIVE DISCUSSION

Metrics/ Methods	KGCNN	CGAN	SSDRNet	Ex_GADerain
SSIM	0.9612	0.8102	0.8054	0.9923
PSNR	26.2464	26.1891	26.087	26.7052
RMSE	1.7125	1.8023	1.9875	0.9367
DSSIM	0.0201	0.0942	0.0987	0.0051

The analysis depicts the enhanced performance of the Ex\_GADerain method based on various assessment measures. Rain streak removal using the Ex\_GADerain utilizes the detail layer extraction for smoothing the rainy image. It also reduces the error through the guided filtering technique. The SA-CCapBiNet-based generator in generating fake images by removing the rain streaks. Here, the proposed SA-CCapBiNet reconstructs the de-rained image through the enhanced capability of feature representation. Also, the consideration of long term dependencies among the information enhances the rain streak removal capability of the model by solving the vanishing gradient issues. Besides, the texture and colour

information maintenance during the rain streaks removal process enhances the quality of a derained image. Considering mean absolute error with the adversarial error for evaluating the loss function minimizes the information learning and makes the generalization more efficient. Thus, the quality assessment of the derained image and the classification tasks acquired better performance.

### V. CONCLUSION

Rain streaks removal using the proposed Ex\_GADerain from the rainy image accurately reconstructed the derained image. The proposed SA-CCapBiNet-based generator enhances the deraining process by considering the long-term dependencies and the generated features' past information. Also, the weight updation based on the dynamic routing of a convolutional capsule network enhances the efficiency of rain streak removal through the neuron vector instead of a single neuron. The self-attention criteria weight the more appropriate features with higher weights, making the rain streak removal more efficient. The quality assessment of the derained image based on various assessment measures like SSIM, PSNR, RMSE, and DSSIM improved performance compared to the conventional rain streak removal methods. The maximal SSIM and PSNR acquired by the Ex\_GADerain are 0.9923 and 26.7052, respectively. The minimal RMSE and DSSIM acquired by the Ex\_GADerain are 0.9367 and 0.0051, respectively. However, the error evaluated by the proposed method is higher. Hence, in the future, a novel rain streak removal method with optimized deep learning will be designed for handling bad rainy conditions

### REFERENCES

- [1] H. Wang, Y. Wu, Q. Xie, Q. Zhao, Y. Liang, S. Zhang, D. Meng, "Single image rain streaks removal: a review and an exploration," International Journal of Machine Learning and Cybernetics, vol. 11, pp. 853-872, 2020.
- [2] Y. Ding, M. Li, T. Yan, F. Zhang, Y. Liu, R. W. Lau, "Rain streak removal from light field images," IEEE Transactions on Circuits and Systems for Video Technology, vol. 32, no. 2, pp.467-482, 2021.
- [3] Y. Shen, Y. Wang, M. Wei, H. Chen, H. Xie, G. Cheng, and F.L. Wang, Semi-MoreGAN: A New Semi-supervised Generative Adversarial Network for Mixture of Rain Removal 2022. arXiv preprint arXiv:2204.13420.
- [4] L. Zhu, Z. Deng, X. Hu, H. Xie, X. Xu, J. Qin, P. A. Heng, "Learning gated nonlocal residual for single-image rain streak removal," IEEE Transactions on Circuits and Systems for Video Technology vol. 31, no. 6, pp.2147-2159, 2020.
- [5] K. Zhang, D. Li, W. Luo, W. Ren, B. Stenger, W. Liu, M. H. Yang, "Dual attention-in-attention model for joint rain streak and raindrop removal," IEEE Transactions on Image Processing vol. 30, pp.7608-7619, 2021.
- [6] T. Yan, M. Li, B. Li, Y. Yang, and R.W.H. Lau, "Rain Removal from Light Field Images with 4D Convolution and Multi-scale Gaussian Process." 2022 arXiv preprint arXiv:2208.07735.
- [7] H. Fazlali, S. Shirani, M. Bradford, T. Kirubarajan, "Single image rain/snow removal using distortion type information," Multimedia Tools and Applications vol. 81, no. 10, pp. 14105-14131, 2022.
- [8] N. Ahn, S. Y.Jo, S. J. Kang, "Eagnet: Elementwise attentive gating network-based single image de-raining with rain simplification," IEEE Transactions on Circuits and Systems for Video Technology vol. 32, no. 2, pp. 608-620, 2021.
- [9] Y. Wei, Z. Zhang, Y. Wang, M. Xu, Y. Yang, S. Yan, M. Wang, "Deraincyclegan: Rain attentive cyclegan for single image deraining and

- rainmaking," IEEE Transactions on Image Processing vol. 30, pp. 4788-4801, 2021.
- [10] D. T. Vu, J. L. Gonzalez, M. Kim, "Exploiting global and local attentions for heavy rain removal on single images," arXiv preprint arXiv: 2104.08126 2021.
- [11] X. Fu, J. Huang, X. Ding, Y. Liao, J. Paisley, "clearing the skies: A deep network architecture for single-image rain removal." IEEE Transactions on Image Processing vol. 26, no. 6, pp. 2944-2956, 2017.
- [12] S. Du, Y. Liu, M. Zhao, Z. Shi, Z. You, and J. Li. "A comprehensive survey: Image deraining and stereo-matching task-driven performance analysis." IET Image Processing vol. 16, no. 1, pp. 11-28, 2022.
- [13] W. Yang, R. T. Tan, S. Wang, Y. Fang, J. Liu, "Single image deraining: From model-based to data-driven and beyond." IEEE Transactions on pattern analysis and machine intelligence vol. 43, no. 11, pp. 4059-4077, 2020.
- [14] X. Hu, L. Zhu, T. Wang, C.W. Fu, P.A. Heng, "Single-image real-time rain removal based on depth-guided nonlocal features," IEEE Transactions on Image Processing vol. 30, pp.1759-1770, 2021.
- [15] P. Li, J. Tian, Y. Tang, G. Wang, C. Wu, Model-based deep network for single image deraining, IEEE Access vol. 8, pp. 14036-14047, 2020.
- [16] K. H. Lee, E. Rvu, J. O. Kim. "Progressive rain removal via a recurrent convolutional network for real rain videos," IEEE Access vol. 8, pp. 203134-203145, 2020.
- [17] X. Fu, Q. Qi, Z. Zha, X. Ding, F. Wu, J. Paisley, "Successive graph convolutional network for image de-raining," International Journal of Computer Vision vol. 129, pp. 1691-1711, 2021.
- [18] L. Cai, Y. Fu, W. Huo, Y. Xiang, T. Zhu, Y. Zhang, H. Zeng, and D. Zeng, "Multi-scale Attentive Image De-raining Networks via Neural Architecture Search." IEEE Transactions on Circuits and Systems for Video Technology 2022.
- [19] Y. Yu, W. Yang, Y. P. Tan, A.C. Kot, "towards robust rain removal against adversarial attacks: A comprehensive benchmark analysis and beyond," In Proceedings of the IEEE/CVF Conference on Computer Vision and Pattern Recognition pp. 6013-6022, 2022.
- [20] Frants, V., Agaian, S., & Panetta, K, "QSAM-Net: Rain streak removal by quaternion neural network with self-attention module," 2022 arXiv preprint arXiv: 2208.04346.
- [21] Y. T. Wang, X. L. Zhao, T. X. Jiang, L. J. Deng, Y. Chang, T. Z. Huang, "Rain streaks removal for single image via kernel-guided convolutional neural network." IEEE Transactions on Neural Networks and Learning Systems vol. 32, no. 8, pp. 3664-3676, 2020.
- [22] C.Y. Lin, Z. Tao, A. S. Xu, L. W. Kang, F. Akhyar, "Sequential dual attention network for rain streak removal in a single image," IEEE Transactions on Image Processing vol. 29, 9250-9265, 2020.
- [23] P. Hettiarachchi, R. Nawaratne, D. Alahakoon, D. De Silva, N. Chilamkurti, "Rain streak removal for single images using conditional generative adversarial networks," Applied Sciences vol. 11, no. 5, pp. 2214, 2021.
- [24] I.J. Jacob, P. E. Darney, "Rain Streaks Removal in digital images by Dictionary based sparsity process with MCA Estimation." Journal of Innovative Image Processing vol. 3, no. 3, pp. 174-189, 2021.
- [25] Y. Chang, M. Chen, C. Yu, Y. Li, L. Chen, L. Yan, "Direction and Residual Awareness Curriculum Learning Network for Rain Streaks Removal," IEEE Transactions on Neural Networks and Learning Systems 2023.
- [26] W. Yang, S. Wang, D. Xu, X. Wang and J. Liu, Towards scale-free rain streak learning via self-supervised fractal band learning. In Proceedings of the AAAI Conference on Artificial Intelligence Vol. 34, No. 07, pp. 12629-12636, 2020, April.
- [27] X. Wang, Z. Li, H. Shan, Z. Tian, Y. Ren, and W. Zhou, "Fastderainnet: A deep learning algorithm for single image deraining." IEEE Access vol. 8, pp. 127622-127630, 2020.
- [28] W. Ran, B. Yang, P. Ma, and H. Lu, "TRNR: Task-Driven Image Rain and Noise Removal With a Few Images Based on Patch Analysis." IEEE Transactions on Image Processing vol. 32, pp. 721-736, 2023.
- [29] Y. Wang, X. Yan, Y. Niu, L. Gong, Y. Guo, and M. Wei, "Joint Depth Estimation and Mixture of Rain Removal From a Single Image." 2023 arXiv preprint arXiv:2303.17766.
- [30] Rainy Image Dataset, <https://drive.google.com/file/d/10cu6MA4fQ2Dz16zfyZrQWDDhOWhRdhpq/view>
- [31] T. Joel, R. Sivakumar, "Nonsampled contourlet transform with cross-guided bilateral filter for despeckling of medical ultrasound images." International Journal of Imaging Systems and Technology vol. 31, no. 2, pp. 763-777, 2021.
- [32] H. H. N. Alrashedy, A. F. Almansour, D. M. Ibrahim, M. A. A. Hammoudeh, "BrainGAN: Brain MRI Image Generation and Classification Framework Using GAN Architectures and CNN Models," Sensors vol. 22, no. 11, pp. 4297, 2022.